Surface anisotropy induced spin wave nonreciprocity in epitaxial La0.33 Sr0.67 MnO3 film on SrTiO3 substrate

Zhang, Jianyu; Burema, Arjan; Chen, Jilei; Hu, Junfeng; Guo, Chenyang; Wang, Hanchen; Li, Ningsheng; Wei, Bohang; Han, Xiufeng; Banerjee, Tamalika

Published in:
Applied Physics Letters

DOI:
10.1063/5.0032552

Applied Physics Letters

Surface anisotropy induced spin wave nonreciprocity in epitaxial $La_{0.33}Sr_{0.67}MnO_3$ film on $SrTiO_3$ substrate

Cite as: Appl. Phys. Lett. **117**, 232402 (2020); https://doi.org/10.1063/5.0032552
Submitted: 09 October 2020 . Accepted: 18 November 2020 . Published Online: 07 December 2020

Jianyu Zhang, Arjan Auke Burema, Jilei Chen, Junfeng Hu, Chenyang Guo, Hanchen Wang, Ningsheng Li, Bohang Wei, Xiufeng Han, Tamalika Banerjee, and Haiming Yu

Applied Physics Letters ARTICLE scitation.org/journal/apl

Surface anisotropy induced spin wave nonreciprocity in epitaxial $La_{0.33}$ $Sr_{0.67}$ MnO_3 film on $SrTiO_3$ substrate

Cite as: Appl. Phys. Lett. **117**, 232402 (2020); doi: 10.1063/5.0032552
Submitted: 9 October 2020 · Accepted: 18 November 2020 ·
Published Online: 7 December 2020

View Online Export Citation CrossMark

Jianyu Zhang,[1] Arjan Auke Burema,[2] Jilei Chen,[1] Junfeng Hu,[1] Chenyang Guo,[3] Hanchen Wang,[1] Ningsheng Li,[1] Bohang Wei,[1] Xiufeng Han,[3] Tamalika Banerjee,[2,a)] and Haiming Yu[1,a)]

AFFILIATIONS

[1]Fert Beijing Institute, School of Microelectronics, Beijing Advanced Innovation Center for Big Data and Brain Computing, Beihang University, Beijing 100191, China
[2]University of Groningen, Zernike Institute for Advanced Materials, 9747 AG Groningen, The Netherlands
[3]Beijing National Laboratory for Condensed Matter Physics, Institute of Physics, University of Chinese Academy of Sciences, Chinese Academy of Sciences, Beijing 100190, China

[a)]**Authors to whom correspondence should be addressed:** t.banerjee@rug.nl and haiming.yu@buaa.edu.cn

ABSTRACT

Spin wave propagation in perovskite $La_{0.33}$ $Sr_{0.67}$ MnO_3 films epitaxially grown on a $SrTiO_3$ substrate of (001) orientation was investigated using an all electrical spin wave spectroscopy technique. The spin wave nonreciprocity in amplitude, resonance frequency, and group velocity of the transmission spectra were observed. The origin of the spin-wave nonreciprocity is attributed to the out-of-plane surface anisotropy, with a value of 1.3 mJ/m^2 at the interface with the substrate, as extracted from the theoretical model. The magnetic field dependence of the frequency shift is attributed to the perpendicular surface anisotropy. The important role of the surface anisotropy in the spin wave nonreciprocity was further confirmed by the angle dependent measurements of the spin wave transmission spectra.

Perovskite $La_{0.33}$ $Sr_{0.67}$ MnO_3 (LSMO) has been studied for its colossal magnetoresistance (CMR) effect since the 1990s.[1,2] Recently, perovskite LSMO is attracting more and more interest in the field of spintronics due to recent observations of the electric field tunability of the magnetoresistance, spin Seebeck effect, and critical temperature of magnetic phase transitions.[3–10] Moreover, epitaxial LSMO on a $SrTiO_3$ (STO) substrate is also attractive for the study of spin wave transmission[11–14] due to its low Gilbert damping[15] of $\alpha \sim 10^{-4}$ and low lattice mismatch with the substrate, which make it a promising candidate for a spin wave transmission study.[16] Spin waves possess interesting characteristics such as high-speed information processing due to their high frequency up to THz and their fairly low energy consumption due to the absence of charge current.[17–24] In view of the above useful properties of LSMO, it is fascinating to explore the possibility of spin wave based information processing in LSMO.[25–37]

Thanks to the development of the spin wave measurement technologies,[36] all electrical spin wave spectroscopy measurements can be conducted with high frequency resolution employing a vector network analyzer (VNA). Spin wave nonreciprocity, which is important for logic device applications,[38] is often used to characterize the magnetic asymmetry in ferromagnetic thin films, in particular the interfacial Dzyaloshinskii–Moriya interaction (DMI), via the frequency and group velocity nonreciprocities.[39,40] When the magnetic films become thick, the DMI induced non-reciprocity will no longer dominate. In this work, we investigate the magnetic field strength and angle dependence of the spin wave spectra on a 139 nm-thick LSMO film grown by pulsed laser deposition on the STO (001) substrate. We observed nonreciprocity in the amplitude, frequency, and group velocity from the spin wave transmission spectra.

The STO substrate was TiO_2-terminated and annealed using an established protocol.[6] After termination, the thin film of LSMO was grown using pulsed laser deposition.[41,42] Our system uses a KrF (248 nm) laser. Before the film deposition, the substrate was heated to 750 °C, with a background pressure of 0.35 mbar of pure oxygen. The laser fluence was set to 2 J/cm^2 and the repetition rate to 1 Hz. The film growth was monitored by *in situ* Reflection High-Energy Electron Diffraction (RHEED) where the intensity oscillations were traced to a film thickness of 139 nm. The growth curve is shown in Fig. S1 in the

supplementary material. After growth, the film was cooled down in 100 mbar oxygen at a rate of 10 °C/min to room temperature.

The sample was patterned into mesas of 90 μm in width and 400 μm in length using photolithography and ion beam etching. The long edge of the mesas is parallel to the edge of the STO substrate. The coplanar waveguide (CPW) antennas that we used for spin wave excitation and detection were fabricated by electron beam lithography (EBL) followed by e-beam evaporation of Cr (5 nm)/Au (120 nm) and subsequent liftoff with acetone. The CPWs were perpendicular to the long edge of the mesas. The measurement configuration and the device details obtained by scanning electron microscopy (SEM) are illustrated in Figs. 1(a) and 1(b), respectively. The spin wave measurement was conducted by a VNA based all electrical spin wave measurement setup. During the measurement, an in-plane external magnetic field was applied to saturate the magnetic moment, and thereafter, the RF current generated by the VNA was injected into the CPWs via microwave probes. Thus, an alternating magnetic field was generated to excite spin waves in the LSMO film. The external in-plane magnetic field was applied along the y axis with the wave vector k along the x direction; hence, the experiment was conducted in the Damon–Eshbach (DE) configuration. The size of the CPW shown in Fig. 1(b) is 0.4 μm for the width of the signal line and the ground lines, and the gap in between is 1.1 μm. The wavevector distribution is shown in Fig. S2 in the supplementary material. The center-to-center distance of two identical CPWs is 5 μm. Before we pattern the sample, the magnetic hysteresis loop was measured at room temperature using a vibrating sample magnetometer (VSM) to characterize the basic magnetic properties. As shown in Fig. 1(c), the contrast between the in-plane and out-of-plane hysteresis loops shows an expected in-plane anisotropy. The equilibrium axis of in-plane anisotropy is along the [100] crystal orientation of LSMO/STO.[43] From the VSM measurement and the RHEED analysis, we calculated the saturation magnetization M_S to be 360.9 kA/m. The imaginary parts of the transmission spectra S_{12} and S_{21} displayed in Figs. 1(d) and 1(e) are obtained in the DE configuration with the magnetic field sweeping from −150 mT to 150 mT with steps of 2 mT. The zoomed in transmission spectra are shown in Fig. S3 in the supplementary material. Both spectra show bright and dark oscillations, which represent the phase information of the propagating spin waves. In order to quantitatively investigate the nonreciprocity between S_{12} and S_{21}, we extracted the single transmission spectrum at 50 mT in Fig. 1(f) as the white dashed line shown in Figs. 1(d) and 1(e). From the single spectrum, both the amplitude and frequency of the spin wave resonance modes are found to display strong nonreciprocity. As denoted in Fig. 1(f), we take the frequency of the oscillation peak as the resonance frequency, and the amplitude is defined as the difference between the peak and its neighboring valley. The group velocity is obtained using the following formula:

$$v_g = \Delta f \cdot s, \tag{1}$$

where Δf is defined as the frequency difference of two neighboring valleys in the oscillation, as illustrated in Fig. 1(f), where s is the center-to-center distance of the two CPWs; here, it is 5 μm.

For a quantitative investigation into the spin wave nonreciprocity, the frequency and group velocity of the spin wave were extracted from the transmission spectrum as shown in Fig. 2. The resonance frequency of S_{12} and S_{21} vs the magnetic field follows the dispersion relation,

$$f = \frac{\gamma\mu_0}{2\pi}\sqrt{(H_{ext} + 4\pi M_S P_k)(H_{ext} - H_A + 4\pi M_S(1 - P_k))} + f_{ani}, \tag{2}$$

where γ is the gyromagnetic ratio, H_{ext} is the external magnetic field, M_S is the saturation magnetization, P_k is the dynamic dipole field

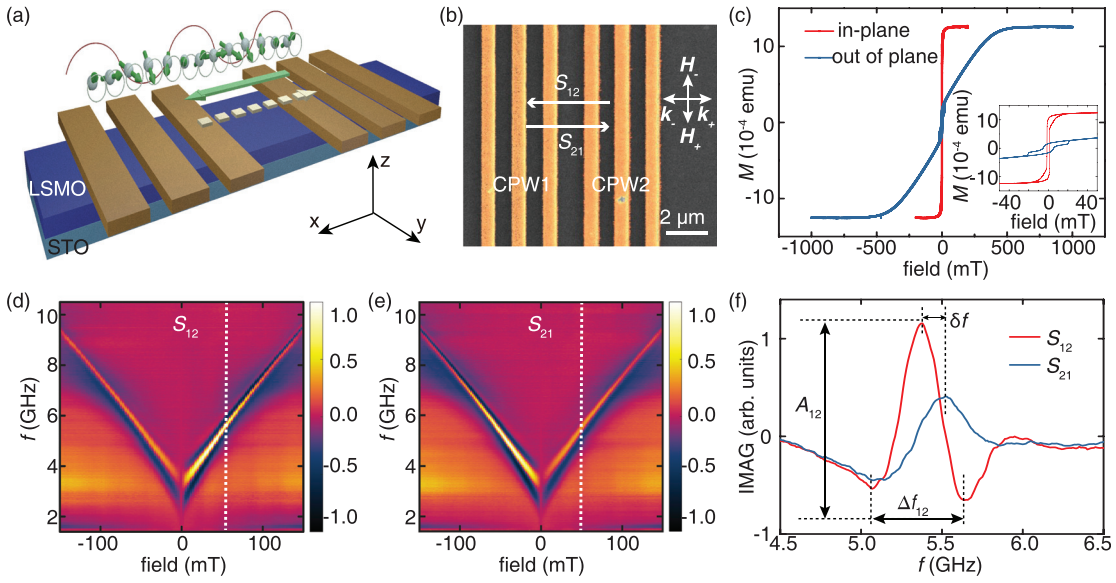

FIG. 1. (a) Sketch of the measurement configuration. Two identical CPWs are used for excitation and detection of spin waves. (b) SEM image of the CPW antennas and the corresponding magnetic field direction. (c) In-plane and out-of-plane magnetic hysteresis loops of the LSMO film. (d) and (e) The transmission spectra S_{12} and S_{21} in the DE configuration, and the magnetic field was swept from negative to positive. (f) The single transmission spectra S_{12} and S_{21} at 50 mT, where a strong nonreciprocity in both amplitude and frequency is observed.

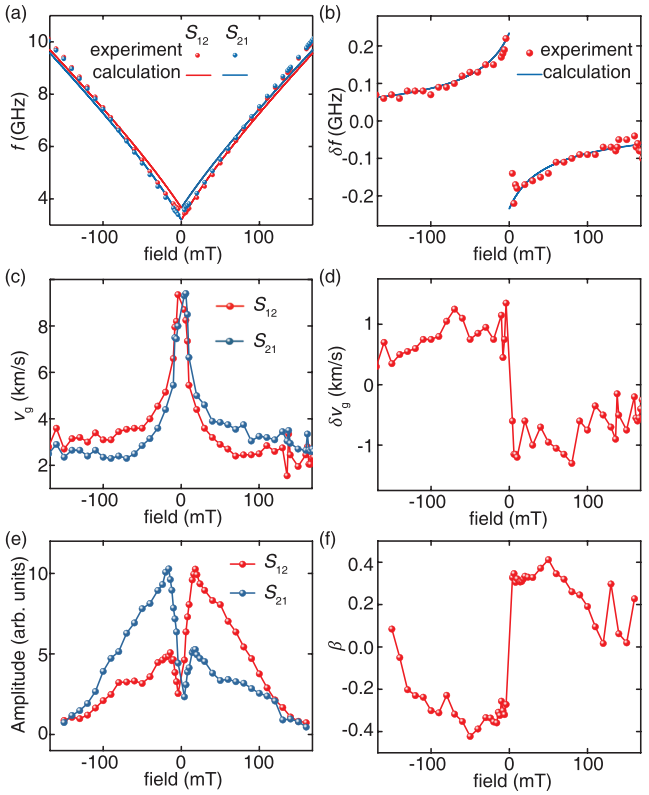

FIG. 2. (a) The extracted spin wave frequency f (dots) and the theoretical model (solid lines) of S_{12} (red) and S_{21} (blue). (b) The frequency shift $\delta f = f_{12} - f_{21}$ experimental data (dots) and the contribution of anisotropy (solid lines). (c) Extracted group velocity v_g of the spin wave transmission spectrum at different magnetic fields and (d) group velocity difference δv_g between S_{12} and S_{21}. (e) The linearized amplitude of the spin wave transmission spectrum. The S_{12} and S_{21} spectra show a maximum at ±18 mT. (f) The amplitude nonreciprocity between S_{12} and S_{21} derived from (e).

factor defined as $P_k = 1-(1-\exp(-|kt|))/|kt|$,[40] t is the thickness of the ferromagnetic LSMO film, k is the wave vector, and H_A is the anisotropy field. The anisotropy induced frequency f_{ani} and the definition of the parameters can be expressed as[44]

$$f_{ani} = \delta Q \frac{\Omega_z^1 - \Omega_z^0}{\Omega_1^2 - \Omega_0^2} \frac{\gamma p \mu_0 M_S}{2\pi}, \tag{3}$$

$$\begin{aligned} \Omega_x^0 &= 1 - P_{00} - \varepsilon + h + \Lambda^2 k^2, \\ \Omega_z^0 &= P_{00} + h + \Lambda^2 k^2, \\ \Omega_x^1 &= 1 - P_{11} - 2\varepsilon + h + \Lambda^2 k^2 + \frac{\Lambda^2 \pi^2}{t^2}, \\ \Omega_z^1 &= P_{11} + h + \Lambda^2 k^2 + \frac{\Lambda^2 \pi^2}{t^2}, \end{aligned} \tag{4}$$

$$\Omega_{0,1}^2 = \frac{\Omega_{00}^2 + \Omega_{11}^2}{2} - Q^2 \mp \frac{1}{2}\sqrt{(\Omega_{11}^2 - \Omega_{00}^2)^2 - 4Q^2\left((P_{00} - P_{11})^2 + \frac{\Lambda^4 \pi^4}{t^4}\right)}, \tag{5}$$

where $P_{00} = 1 - \frac{1-e^{-|k|t}}{|k|t}$, $P_{11} = \frac{(kt)^2}{\pi^2+(kt)^2}\left(1 - \frac{2(kt)^2}{\pi^2+(kt)^2}\frac{1+e^{-|k|t}}{|k|t}\right)$, $\varepsilon = \frac{2}{t\mu_0 M_S^2}(K_s^{bot} + K_s^{top})$, $\delta = \frac{2\sqrt{2}}{t\mu_0 M_S^2}(K_s^{bot} - K_s^{top})$, K_s^{bot} and K_s^{top} are the uniaxial out-of-plane surface anisotropy at the bottom (K_s^{bot}) and top (K_s^{top}) surfaces of the LSMO film. $Q = \frac{\sqrt{2}kt}{\pi^2+(kt)^2}(1+e^{-|k|t})$, $\Omega_{00} = \sqrt{\Omega_x^0 \Omega_z^0}$, $\Omega_{11} = \sqrt{\Omega_x^1 \Omega_z^1}$, $h = H/M_S$ is the dimensionless applied field, $\Lambda = (2A/\mu_0 M_S^2)^{1/2}$ is the exchange length, and A is the exchange stiffness constant.

We could account for the data using this model with $\gamma/2\pi = 29.2$ GHz/T, $M_S = 0.45$ T, $k = 1.3$ rad/μm, $t = 139$ nm, $K_s^{bot} = 1.3$ mJ/m^2, which is close to the calculated anisotropy reported previously[45] (1.2 mJ/m^2), $K_s^{top} = 0$ mJ/m^2 for no capping layer on the top, and $A = 1.5 \times 10^{-11}$ J/m in Eq. (2). Good agreement with the experimental results in both the frequency and frequency shift was obtained [Figs. 2(a) and 2(b)]. In Fig. 2(b), the magnetic field dependence of the frequency shift δf and the prediction of the model are plotted. Thus, we find that the shift can be attributed to the surface anisotropy of the magnetic LSMO layer. The anisotropy arises from the lattice mismatch between $La_{0.33}$ $Sr_{0.67}$ MnO_3 ($a = 3.87$ Å)[46] and $SrTiO_3$ ($a = 3.905$ Å),[47] where the tensile strain from the substrate gradually relaxes with the film thickness. The strain difference between the top and bottom surfaces of the LSMO film induces different surface anisotropy values, resulting in the frequency shift between S_{12} and S_{21} of the DE mode spin waves. The static magnetorestriction gives rise to an in-plane anisotropy. However, the dynamic magnetorestriction is not taken into account in the calculation, considering that rather small oscillating magnetic fields[48] are generated by the CPW and the magnon-phonon coupling[49] is weak due to dispersion relations of magnons and phonons in the LSMO being far apart. The group velocity of spin waves is plotted in Fig. 2(c). Both S_{12} and S_{21} show a sharp peak at ~9 km/s near 0 mT and then drop sharply with the increasing external field. There is also a difference in the group velocity between S_{12} and S_{21}. The group velocity difference δv_g is negative in the positive magnetic field direction and vice versa as shown in Fig. 2(d), and the absolute difference shows a slightly decreasing slope with the increasing magnetic field. For the thick film studied in this work, the surface anisotropy is mainly located at the film bottom.[50,51] The anisotropy difference between the top and bottom surfaces may result in spin-wave nonreciprocity[44] for magnetostatic surface waves, i.e., Damon-Eshbach spin waves.

The nonreciprocity in spin-wave group velocity is shown in Figs. 2(c) and 2(d), which can also be interpreted as a result of the surface anisotropy, according to Eq. (1). When the external magnetic field increases, the resonance frequency also increases. However, the intrinsic anisotropy field is constant, and with the increasing external field, the ratio of the anisotropy-induced field to the total effective field becomes small; thus, the anisotropy induced δf and δv_g also become smaller. The magnetic field dependence of the spin wave amplitude is plotted in Fig. 2(e), and the amplitude is seen to increase with the magnetic field and achieves a maximum at around ±18 mT, which is consistent with the in-plane saturation field of the sample as shown in the inset of Fig. 1(c). In the DE mode configuration, the main contribution in the amplitude nonreciprocity is attributed to the surface spin wave mode[52] and the surface anisotropy. The field dependence of the amplitude non-reciprocity between S_{12} and S_{21} is shown in Fig. 2(f), where

the sign changes at zero field due to the reverse of the external magnetic field.

After the investigation of the magnetic field strength dependence in the DE configuration, we also conducted measurements of the transmission spectrum with the angular dependence of the magnetic field as shown in Fig. 3. Here, θ is defined as the angle between the wave vector $\boldsymbol{k}$ and the external magnetic field $\boldsymbol{H}$; $\theta = \pm 90°$ ($\boldsymbol{k} \perp \boldsymbol{H}$), which corresponds to the DE configuration where the spin wave propagates along the bottom and top surfaces of the magnetic film, and $\theta = \pm 180°$ or $0°$ ($\boldsymbol{k} \parallel \boldsymbol{H}$), which corresponds to the backward volume (BV) mode configuration where the spin wave propagates in the volume of the magnetic film.[53] The measurement was conducted under a fixed magnetic strength of 50 mT with the magnetic field direction rotating from $-180°$ to $180°$, and for each angle, a spin wave transmission spectrum was obtained. From the spectrum, we observe a strong angle dependence of the spin wave signals. The oscillation in the transmission spectrum mainly appears at around $\pm 90°$ when $k \perp H$, that is, when the DE mode spin waves are excited. In the angle dependence measurements, the magnetization in LSMO rotates with the external field. When the field angle θ deviates from, $\pm 90°$ or $0°, 180°$, the magnetization in LSMO will have projections in both orthogonal directions, parallel and perpendicular to the wavevector $\boldsymbol{k}$. In such a configuration, spin waves of both the DE mode and BV mode can be excited. When the magnetization rotates from $\theta = 90°$ to $\theta = 0°$, the spin wave mode changes from the DE spin waves (surface mode) to BV spin waves (volume mode) progressively.[24,54,55] As a result, the surface anisotropy-induced spin wave nonreciprocity maximizes at $\theta = 90°$ (DE mode) and gradually reduces toward $\theta = 0°$ (BV mode) as observed in the angle-dependent measurement shown in Figs. 3(c) and 3(d). This further confirms the important role of the surface anisotropy on the amplitude and frequency nonreciprocity. More detailed angle dependence measurement data can be found in Fig. S4 of the supplementary material, where the field dependence of spin wave transmission spectra was taken at different angles and major changes in the spin wave spectra were observed.

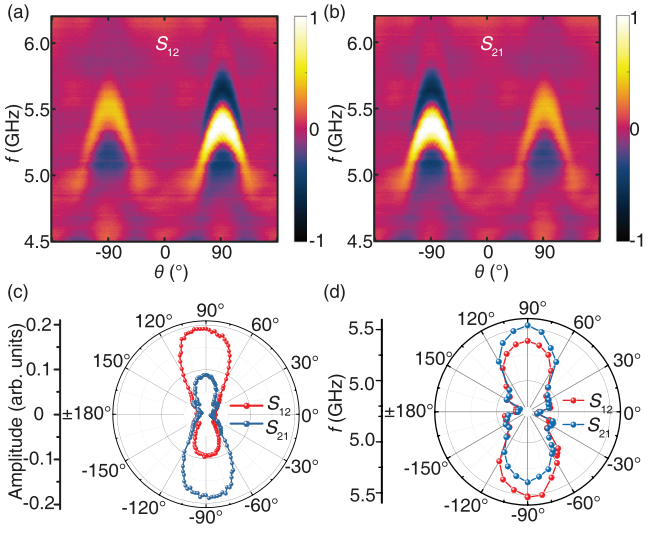

FIG. 3. The magnetic field angle dependence of the transmission spectrum at 50 mT. The angle θ in S_{12} (a) and S_{21} (b) is defined as the angle between the wavevector and the external magnetic field. The amplitude and the frequency of the spin waves vs θ are plotted in (c) and (d), respectively.

In summary, we studied the magnetic field dependence, in both strength and direction, of the propagation of spin wave spectra and observed transmission oscillation in the DE configuration. Furthermore, by fitting the experimental data with a theoretical model, a strong surface anisotropy constant of 1.3 mJ/m^2 was deduced. The anisotropy plays a dominant role in the spin wave frequency nonreciprocity, group velocity, and amplitude. This is further confirmed by the magnetic field angle dependent measurement, which is relevant for the application of spin wave based devices using LSMO. It will be interesting to study the thickness dependence of the spin wave spectra since for thinner LSMO films, the interaction with the substrate will modify the magnetic anisotropy, leading to differences in the spin wave spectrum.

See the supplementary material for detailed information about the film growth, fabricated device, and spin wave measurements in different magnetic field directions.

AUTHORS' CONTRIBUTIONS

J.Z., A.A.B., and J.C. contributed equally to this work.

We thank Jinxing Zhang, Shizhe Wu, Yuelin Zhang, and Jean-Philippe Ansermet for helpful discussions. Financial support by NSF China under Grant Nos. 11674020 and U1801661, the 111 talent program B16001, and the National Key Research and Development Program of China under Grant Nos. 2016YFA0300802 and 2017YFA0206200 is gratefully acknowledged. This work is realized using NanoLab NL facilities and is a part of the research program Skyrmionics: Toward New magnetic Skyrmions and Topological Memory (Project No. 16SKYR04). A.A.B acknowledges financial support from the Netherlands Organisation for Scientific Research (NWO).

DATA AVAILABILITY

The data that support the findings of this study are available within the article and its supplementary material and are available from the corresponding authors on reasonable request.

REFERENCES

[1]J. Fontcuberta, B. Martínez, A. Seffar, S. Piñol, J. L. García-Muñoz, and X. Obradors, Phys. Rev. Lett. **76**, 1122 (1996).
[2]Y. Lu, X. W. Li, G. Q. Gong, and G. Xiao, Phys. Rev. B **54**, R8357 (1996).
[3]B. W. Wu, G. Y. Luo, J. G. Lin, and S. Y. Huang, Phys. Rev. B **96**, 060402 (2017).
[4]C. Liu, S. Wu, J. Zhang, J. Chen, J. Ding, J. Ma, Y. Zhang, Y. Sun, S. Tu, H. Wang, P. Liu, C. Li, Y. Jiang, P. Gao, D. Yu, J. Xiao, R. Duine, M. Wu, C.-W. Nan, J. Zhang, and H. Yu, Nat. Nanotechnol. **14**, 691 (2019).
[5]J. Wang, S. Wu, J. Ma, L. Xie, C. Wang, I. A. Malik, Y. Zhang, K. Xia, C.-W. Nan, and J. Zhang, Appl. Phys. Lett. **112**, 072408 (2018).
[6]A. Das, S. T. Jousma, and T. Banerjee, SPIN **8**, 1840004 (2018).
[7]M. Zhu, Z. Zhou, X. Xue, M. Guan, D. Xian, C. Wang, Z. Hu, Z.-D. Jiang, Z.-G. Ye, W. Ren, and M. Liu, Appl. Phys. Lett. **111**, 102903 (2017).
[8]J. Z. Sun, D. W. Abraham, R. A. Rao, and C. B. Eom, Appl. Phys. Lett. **74**, 3017 (1999).
[9]A. M. Kamerbeek, R. Ruiter, and T. Banerjee, Sci. Rep. **8**, 1378 (2018).
[10]S. E. Lofland, V. Ray, P. H. Kim, and S. M. Bhagat, Phys. Rev. B **55**, 2749 (1997).

[11]R. Magaraggia, M. Hambe, M. Kostylev, V. Nagarajan, and R. L. Stamps, Phys. Rev. B **84**, 104441 (2011).
[12]A. Ettayfi, R. Moubah, E. K. Hlil, S. Colis, M. Lenertz, A. Dinia, and H. Lassri, J. Magn. Magn. Mater. **409**, 34 (2016).
[13]G. Inkoom, F. Boakye, and J. Archer, Res. J. Appl. Sci. Eng. Technol. **7**(15), 3064 (2014).
[14]E. Wahlström, F. Macià, F. Macià, J. E. Boschker, Å. Monsen, P. Nordblad, R. Mathieu, A. D. Kent, and T. Tybell, New J. Phys. **19**, 063002 (2017).
[15]Q. Qin, S. He, W. Song, P. Yang, Q. Wu, Y. P. Feng, and J. Chen, Appl. Phys. Lett. **110**, 112401 (2017).
[16]A. Vailionis, H. Boschker, Z. Liao, J. R. A. Smit, G. Rijnders, and M. Huijben, Appl. Phys. Lett. **105**, 131906 (2014).
[17]H. Yu, O. d'Allivy Kelly, V. Cros, R. Bernard, P. Bortolotti, A. Anane, F. Brandl, R. Huber, I. Stasinopoulos, and D. Grundler, Sci. Rep. **4**, 6848 (2014).
[18]V. V. Kruglyak, S. O. Demokritov, and D. Grundler, J. Phys. D: Appl. Phys. **43**, 264001 (2010).
[19]B. Lenk, H. Ulrichs, F. Garbs, and M. Münzenberg, Phys. Rep. **507**, 107–136 (2011).
[20]A. V. Chumak, V. I. Vasyuchka, A. A. Serga, and B. Hillebrands, Nat. Phys. **11**, 453–461 (2015).
[21]V. E. Demidov, S. Urazhdin, G. de Loubens, O. Klein, V. Cros, A. Anane, and S. O. Demokritov, Phys. Rep. **673**, 1–31 (2017).
[22]G. Csaba, A. Papp, and W. Porod, Phys. Lett. A **381**, 1471 (2017).
[23]A. Khitun, M. Q. Bao, and K. L. Wang, J. Phys. D: Appl. Phys. **43**(26), 264005 (2010).
[24]B. A. Kalinikos and A. N. Slavin, J. Phys. C **19**, 7013 (1986).
[25]Y. Wang, D. Zhu, Y. Yang, K. Lee, R. Mishra, G. Go, G. Go, D. Kim, K. Cai, E. Liu *et al.*, Science **366**, 1125 (2019).
[26]J. Han, P. Zhang, J. T. Hou, S. A. Siddiqui, and L. Liu, Science **366**, 1121 (2019).
[27]K. Wagner, A. Kákay, K. Schultheiss, A. Henschke, T. Sebastian, and H. Schultheiss, Nat. Nanotechnol. **11**, 432–436 (2016).
[28]S. J. Hämäläinen, M. Madami, H. Qin, G. Gubbiotti, and S. van Dijken, Nat. Commun. **9**, 4853 (2018).
[29]A. Haldar, D. Kumar, and A. O. Adeyeye, Nat. Nanotechnol. **11**, 437–443 (2016).
[30]L. J. Cornelissen, J. Liu, R. A. Duine, J. Ben Youssef, and B. J. van Wees, Nat. Phys. **11**, 1022–1026 (2015).
[31]Q. Wang, P. Pirro, R. Verba, A. Slavin, B. Hillebrands, and A. V. Chumak, Sci. Adv. **4**, e1701517 (2018).
[32]C. Liu, J. Chen, T. Liu, F. Heimbach, H. Yu, Y. Xiao, J. Hu, M. Liu, H. Chang, T. Stueckler, S. Tu, Y. Zhang, Y. Zhang, P. Gao, Z. Liao, D. Yu, K. Xia, N. Lei, W. Zhao, and M. Wu, Nat. Commun. **9**, 738 (2018).
[33]S. Wintz, V. Tiberkevich, M. Weigand, J. Raabe, J. Lindner, A. Erbe, A. Slavin, and J. Fassbender, Nat. Nanotechnol. **11**, 948–953 (2016).
[34]S.-M. Seo, K.-J. Lee, H. Yang, and T. Ono, Phys. Rev. Lett. **102**, 147202 (2009).
[35]V. Vlaminck and M. Bailleul, Phys. Rev. B **81**, 014425 (2010).
[36]V. Vlaminck and M. Bailleul, Science **322**, 410–413 (2008).
[37]Y. Kajiwara, K. Harii, S. Takahashi, J. Ohe, K. Uchida, M. Mizuguchi, H. Umezawa, H. Kawai, K. Ando, K. Takanashi, S. Maekawa, and E. Saitoh, Nature **464**, 262–266 (2010).
[38]M. Jamali, J. Hyun Kwon, S.-M. Seo, K.-J. Lee, and H. Yang, Sci. Rep. **3**, 3160 (2013).
[39]H. Wang, J. Chen, T. Liu, J. Zhang, K. Baumgaertl, C. Guo, Y. Li, C. Liu, P. Che, S. Tu, S. Liu, P. Gao, X. Han, D. Yu, M. Wu, D. Grundler, and H. Yu, Phys. Rev. Lett. **124**, 027203 (2020).
[40]J. M. Lee, C. Jang, B.-C. Min, S.-W. Lee, K.-J. Lee, and J. Chang, Nano Lett. **16**, 62–67 (2016).
[41]A. A. Burema, J. J. L. van Rijn, and T. Banerjee, J. Vac. Sci. Technol. **37**(2), 021103 (2019).
[42]K. G. Rana, S. Parui, and T. Banerjee, Phys. Rev. B **87**, 085116 (2013).
[43]Y. Suzuki, H. Y. Hwang, S. W. Cheong, and R. B. van Dover, Appl. Phys. Lett. **71**, 140 (1997).
[44]O. Gladii, M. Haidar, Y. Henry, M. Kostylev, and M. Bailleul, Phys. Rev. B **93**, 054430 (2016).
[45]H. K. Lee, I. Barsukov, A. G. Swartz, B. Kim, L. Yang, H. Y. Hwang, and I. N. Krivorotov, AIP Adv. **6**, 055212 (2016).
[46]M. C. Martin, G. Shirane, Y. Endoh, K. Hirota, Y. Moritomo, and Y. Tokura, Phys. Rev. B **53**, 14285 (1996).
[47]H. Boschker, M. Huijben, A. Vailionis, J. Verbeeck, S. van Aert, M. Luysberg, S. Bals, G. van Tendeloo, E. P. Houwman, and G. Rijnders, J. Phys. D: Appl. Phys. **44**, 205001 (2011).
[48]S. Zhang, X. Dong, Y. Chen, G. Wang, J. Zhu, and X. Tang, Solid State Commun. **151**, 982–984 (2011).
[49]X. Zhang, G. E. W. Bauer, and T. Yu, Phys. Rev. Lett. **125**, 077203 (2020).
[50]G. Bochi, C. A. Ballentine, H. E. Inglefield, C. V. Thompson, R. C. O'Handley, H. J. Hug, B. Stiefel, A. Moser, and H.-J. Güntherodt, Phys. Rev. B **52**, 7311 (1995).
[51]S. Ikeda, K. Miura, H. Yamamoto, K. Mizunuma, H. D. Gan, M. Endo, S. Kanai, J. Hayakawa, F. Matsukura, and H. Ohno, Nat. Mater. **9**, 721–724 (2010).
[52]K. L. Wong, L. Bi, M. Bao, Q. Wen, J. P. Chatelon, Y. Lin, C. A. Ross, H. Zhang, and K. L. Wang, Appl. Phys. Lett. **105**, 232403 (2014).
[53]T. Schneider, A. A. Serga, T. Neumann, B. Hillebrands, and M. P. Kostylev, Phys. Rev. B **77**, 214411 (2008).
[54]D. D. Stancil and A. Prabhakar, *Spin Waves: Theory and Applications. Appendix C* (Springer, 2009).
[55]H. Yu, G. Duerr, R. Huber, M. Bahr, T. Schwarze, F. Brandl, and D. Grundler, Nat. Commun. **4**, 2702 (2013).